Electromagnetic Absorption in the Human Head and Neck for Mobile Telephones at 835 and 1900 MHz

Om P. Gandhi, *Fellow, IEEE*, Gianluca Lazzi, *Member, IEEE*, and Cynthia M. Furse, *Member, IEEE*

Abstract— **We have used the finite-difference time-domain method and a new millimeter-resolution anatomically based model of the human to study electromagnetic energy coupled to the head due to mobile telephones at 835 and 1900 MHz. Assuming reduced dimensions characteristic of today's mobile telephones, we have obtained SAR distributions for two different lengths of monopole antennas of lengths $\lambda/4$ and $3\lambda/8$ for a model of the adult male and reduced-scale models of 10- and 5-year-old children and find that peak one-voxel and 1-g SAR's are larger for the smaller models of children, particularly at 835 MHz. Also, a larger in-depth penetration of absorbed energy for these smaller models is obtained. We have also studied the effect of using the widely disparate tissue properties reported in the literature and of using homogeneous instead of the anatomically realistic heterogeneous models on the SAR distributions. Homogeneous models are shown to grossly overestimate both the peak 1-voxel and 1-g SAR's. Last, we show that it is possible to use truncated one-half or one-third models of the human head with negligible errors in the calculated SAR distributions. This simplification will allow considerable savings in computer memory and computation times.**

I. Introduction

CELLULAR telephones and mobile wireless communication systems are being introduced into society at a very rapid rate. This has resulted in public concern about the health hazards of RF electromagnetic fields that are emitted by these devices. In this paper, we describe a study of the electromagnetic absorption in the human body for some typical antennas used for these telephones and compare the mass-normalized rates of energy absorption (specific absorption rates or SAR's) with the ANSI/IEEE C95.1-1992 RF Safety Guidelines [1]. These safety guidelines are given in terms of the maximum permissible exposures (MPE) of electric and magnetic fields, or of power density for controlled and uncontrolled environments. Though simple to use for far-field, relatively uniform exposures, the MPE limits are not easy to use for highly nonuniform fields such as in the near-field region of a cellular telephone. An alternative procedure given in the following [1] has, therefore, been suggested to satisfy the safety guidelines for uncontrolled environments which are defined as situations where there is exposure of individuals who have no knowledge or control of their exposure.

Manuscript received October 6, 1995; revised February 2, 1996.

The authors are with the Department of Electrical Engineering, University of Utah, Salt Lake City, Utah 84112 USA.

Publisher Item Identifier S 0018-9480(96)07034-2.

An exposure condition can be considered to be acceptable if it can be shown that it produces SAR's "below 0.08 W/kg, as averaged over the whole body, and spatial peak SAR values not exceeding 1.6 W/kg, as averaged over any 1 g of tissue (defined as a tissue volume in the shape of a cube)."

For calculations of the SAR distributions we have used the well-established finite-difference time-domain (FDTD) numerical electromagnetic method which has previously been used for a number of bioelectromagnetic problems pertaining to far-field or near-field exposures from ELF to microwave frequencies [2]. We have also used a newly developed millimeter-resolution model of the human body obtained from the magnetic resonance imaging (MRI) scans of a male volunteer. This whole-body model has a resolution of 1.875 mm for the two orthogonal axes in the cross-sectional planes and 3 mm along the height of the body [2]. The head and neck part of this model has previously been used to study SAR distributions for ten commercially available cellular telephones [2], [3] operating at transmission frequencies of 820–850 MHz (center frequency of 835 MHz). It has also been used to calculate electromagnetic absorption in the human head for some experimental handheld transceivers operating at 6 GHz [4]. This same anatomically based part-body model has also been used for the calculations given in this paper.

We are aware of some recent publications on the SAR calculations for mobile telephones using anatomically based models of the human head [5], [6]. Whereas a somewhat cruder model of the human head with a resolution of 6.56 mm was used in [5], a higher-resolution MRI-based model with 2-mm cell size has been used by Dimbylow and Mann [6] for calculations with $\lambda/4$ monopoles above a metal box and for $\lambda/2$ dipoles.

For calculations reported in this paper we have examined two different lengths of monopole antennas, $\lambda/4$ and $3\lambda/8$, mounted on plastic-coated handsets of dimensions that are typical of newer mobile telephones both at 835 and 1900 MHz. We have also studied the effect of tilting the handset as for typical usage at an angle of 33° relative to vertical and compared the results with the SAR's when the antenna is held vertically relative to the head. By scaling the model of the head and neck to obtain reduced-size models representative of 10- and 5-year-old children, we have calculated the SAR distributions and find deeper penetration of EM energy, and SAR's for internal tissues that are several times higher than

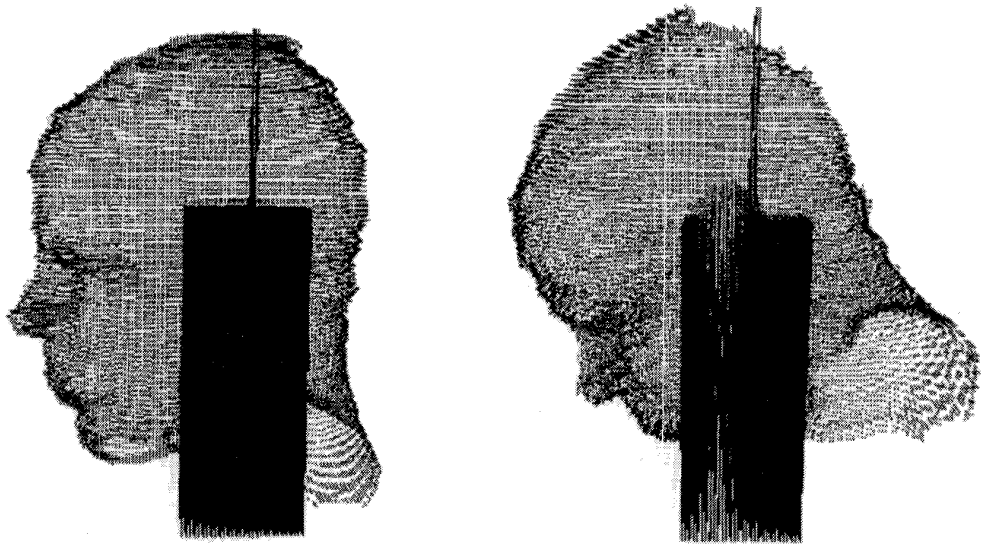

(a) (b)

Fig. 1. The two head models with the telephone used for the calculations: (a) vertical, (b) tilted 30° relative to vertical.

TABLE I

DIELECTRIC PROPERTIES AND SPECIFIC GRAVITIES OF THE VARIOUS TISSUES ASSUMED AT THE MIDBAND MOBILE TELEPHONE FREQUENCIES OF 835 AND 1900 MHz [12]. ALSO INCLUDED ARE THE LOWER DIELECTRIC PROPERTIES FOR FAT, BONE, AND CARTILAGE PREVIOUSLY REPORTED IN THE LITERATURE [14], [16]

		835 MHz		1900 MHz	
Tissue	Spec. Gravity 10^3kg/m^3	ε_r	σ S/m	ε_r	σ S/m
muscle	1.04	51.76	1.11	49.41	1.64
fat	0.92	9.99	0.17	9.38	0.26
bone (skull)	1.81	17.40	0.25	16.40	0.45
cartilage	1.10	40.69	0.82	38.10	1.28
skin	1.01	35.40	0.63	37.21	1.25
nerve	1.04	33.40	0.60	32.05	0.90
blood	1.06	55.50	1.86	54.20	2.27
parotid gland	1.05	45.25	0.92	43.22	1.29
CSF	1.01	78.10	1.97	77.30	2.55
eye humour	1.01	67.90	1.68	67.15	2.14
sclera	1.17	54.90	1.17	52.56	1.73
lens	1.10	36.59	0.51	42.02	1.15
pineal gland	1.05	45.26	0.92	43.22	1.29
pituitary gland	1.07	45.26	0.92	43.22	1.29
brain	1.04	45.26	0.92	43.22	1.29
		Old properties [14, 16]		Old properties [14, 16]	
fat	0.92	7.20	0.16	9.70	0.27
bone (skull)	1.81	7.20	0.16	8.40	0.15
cartilage	1.10	7.20	0.16	9.70	0.27

TABLE II
DIELECTRIC PROPERTIES AND SPECIFIC GRAVITIES ASSUMED FOR TEST RUNS FOR COMPARISON WITH THE CALCULATIONS OF DIMBYLOW AND MANN [6]

Tissue	Spec. Gravity 10^3kg/m^3	835 MHz ε_r	835 MHz σ S/m	1900 MHz ε_r	1900 MHz σ S/m
muscle	1.04	58.00	1.21	56.00	1.76
fat	0.92*	9.99*	0.17*	9.38*	0.26*
bone (skull)	1.85	8.00	0.11	8.00	0.15
cartilage	1.10	35.00	0.60	32.00	0.57
skin	1.10	35.00	0.60	32.00	0.57
nerve	1.04*	33.4*	0.60*	32.05*	0.90*
blood	1.06	64.00	1.24	64.00	1.80
parotid gland	1.05*	45.25*	0.92*	43.22*	1.29*
CSF	1.06	72.00	2.13	72.00	2.50
eye humour	1.01	73.00	1.97	74.00	2.27
sclera	1.01	66.00	1.93	62.00	2.28
lens	1.05	44.00	0.80	42.00	1.19
pineal gland	1.05*	45.26*	0.92*	43.22*	1.29*
pituitary gland	1.07*	45.26*	0.92*	43.22*	1.29*
brain	1.03	49.00	1.10	47.00	1.42

* These values were not prescribed in [6].

for the model of the adult. Since the tissue properties are not as well characterized, and widely varying values have been reported for fat, bone, and cartilage, we have studied the effect that these properties can have on peak 1-g SAR's that need to be examined for compliance with the ANSI/IEEE safety guidelines. We have identified a problem with interpreting the ANSI/IEEE safety guidelines since unspecified and different subvolumes in the shape of a cube may be taken in order to obtain peak 1-g SAR's that should not exceed 1.6 W/kg for uncontrolled environments [1]. For slightly larger subvolumes involving the more superficial regions including the air pockets of the ear, considerably higher 1-g SAR's are obtained. This problem has been temporarily resolved with advice from the Dosimetry Working Group of WTR [see Section IV]. Finally, we have developed a procedure for using smaller truncated models by factors of 2–3 with minimal loss of accuracy in determination of SAR distributions for the exposed region of the head.

II. THE FDTD METHOD

The finite-difference time-domain method has been described in several publications and a couple of recent textbooks [7], [8]. This method has also been used successfully to obtain specific absorption rates for anatomically based models of the human body for whole-body or partial-body exposures to spatially uniform or nonuniform (far-field or near-field) electromagnetic fields from ELF to microwave frequencies [2], [9]. In this method, the coupled Maxwell's equations in differential form are solved for all points of the absorber (model of the human head and neck and the approximate model of the hand), as well as the space including the plastic-coated handset, the antenna embedded in a dielectric sheathing and the region to the absorbing boundaries which are generally taken to be at least 10 cells away from the telephone-head/neck coupled region. For all of the calculations reported in this paper we have used the retarded-time absorbing-boundary condition [10]. The time resolution $\delta t = \delta/2c = 3.29$ ps was taken to correspond to the smaller of the cell dimensions of 1.974 mm. To get converged results, we have used 8 time periods for each of the two frequencies of 835 and 1900 MHz that were used for the SAR distributions. It is recognized that different handset dimensions are being used for the cellular telephones, and the dimensions of the handset do influence the radiated fields and the SAR distribution patterns [11]. We have taken a handset dimension of 2.96 × 5.73 × 15.5 cm typical of today's handsets for most of the calculations given in this paper. This includes a metal box of dimensions $14\delta_x \times 28\delta_y \times 51\delta_z$ (2.76 × 5.53 × 15.3 cm) and 1-cell thickness δ of plastic coating of effective dielectric constant[1] K_e given by the following equation which is somewhat lower than the

[1] The effective dielectric constant K_e is derived by noting that the electric fields close to a metallic surface such as that of a handset are primarily normal and only a part of the FDTD-cell width is actually filled with the dielectric material. The required continuity of the normal component of $D = \varepsilon E$ with the outer region can be used to obtain K_e.

TABLE III
SAR DISTRIBUTIONS FOR THE SQUISHED-EAR MODEL OF THE ADULT MALE FOR $\lambda/4$ AND $3\lambda/8$ ANTENNAS AT 1900 MHz. TIME-AVERAGED RADIATED POWER = 125 mW

	$\lambda/4$ antenna	$3\lambda/8$ antenna
Peak 1-voxel SAR (W/kg)	3.90	2.66
Peak 1-g SAR (W/kg)[1]	0.52 (1.01 g; 98.7%)	0.32 (1.01 g; 98.7%)
Peak 1-g SAR (W/kg)[2]	1.11 (1.03 g; 81.0%)	0.69 (1.06 g; 86.0%)
Peak 1-g SAR (W/kg)[3]	1.03 (1.10 g; 82.4%)	0.69 (1.11 g; 86.1%)
Peak 1-g SAR for brain (W/kg)[2]	0.20 (1.00 g)	0.16 (1.00 g)
Peak 1-g SAR for brain (W/kg)[3]	0.19 (1.05 g)	0.16 (1.00 g)
Power absorbed by head and neck	35.6%	29.4%
Power absorbed by "hand"	13.8%	7.0%
Peak 1-voxel SAR for brain (W/kg)	0.29	0.26
CSF average (mW/kg)	8.0	8.3
Brain average (mW/kg)	7.6	7.6
Humour average (mW/kg)	3.2	2.6
Lens average (mW/kg)	1.5	1.3
Sclera average (mW/kg)	1.8	1.5

[1] $5 \times 5 \times 3$ cells; $0.987 \times 0.987 \times 0.9$ cm; 0.88 cm^3

[2] $5 \times 5 \times 4$ cells; $0.987 \times 0.987 \times 1.2$ cm; 1.17 cm^3

[3] $6 \times 6 \times 3$ cells; $1.184 \times 1.184 \times 0.9$ cm; 1.26 cm^3

It was not possible to obtain 1-g weight of the brain for subvolume 1; hence, the 1-g SAR for brain for this case is not given.

dielectric constant ε_r of the actual insulation layer of thickness w (generally 1 mm).

$$K_e = \frac{\delta//\varepsilon_r}{[\varepsilon_r(\delta - w) + w]} \tag{1}$$

Here δ is the dimension of the Yee cell which may be δ_x, δ_y, or δ_z depending on the surface of the metal handset.

III. A MILLIMETER-RESOLUTION ANATOMIC MODEL OF THE HUMAN BODY

We have recently developed a millimeter-resolution model of the human body from the magnetic resonance imaging (MRI) scans of a male volunteer of height 176.4 cm and weight 64 kg. The MRI scans were taken with a resolution of 3 mm along the height of the body and 1.875 mm for the orthogonal axes in the cross-sectional planes. Even though the height of the volunteer was quite appropriate for an average male, the weight was somewhat lower than an average of 71 kg, which is generally assumed for an average male. This problem can, to some extent, be ameliorated by assuming that the pixel dimensions for the cross sections are larger than 1.875 mm by the ratio of $(71/64)^{1/2} = 1.053$, i.e., 1.974 mm instead of 1.875 mm. Using a software package from the Mayo Clinic called ANALYZE, the MRI scans of the human body were converted into images involving 30 tissue types whose electrical properties (ε_r, σ) can then be prescribed at the mobile telephone midband frequencies of 835 MHz or 1900 MHz. The tissues taken for the whole-body model are: muscle, fat, regular bone, compact bone, cartilage, skin, nerve, intestine, spleen, pancreas, heart, blood, parotid gland, liver, kidney, lung, bladder, cerebrospinal fluid, eye humour, eye sclera, eye lens, stomach, erectile tissue, prostate gland, spermatic cord, testicle, ligament, brain, pineal gland, and pituitary gland. Since only the model of the head and neck is used for the present calculations, only 15 of these tissues are involved in this model. The new dielectric properties assumed for the various tissues at 835 and 1900 MHz are given in Table I. These are taken from the unpublished data of Gabriel [12]. We have considered two orientations of the handset, one that is held vertically relative to the head (tilt angle of 0°) and another that is held at a tilt angle of 30° relative to the head (see Fig. 1). To simulate a handset that is typically tilted forward by 30° for a vertically erect head, we have modified the MRI-based model so that it is tilted forward by 30°. As described in [13], the forward tilt is accomplished by a "best fitting" technique wherein each of the cells of the present model is assigned to a new corresponding cell only if no other cells have a better fitting to the new one. An error matrix proportional to the distance of the rotated cells from the cell centroid of the new cell is used and minimized to obtain the

TABLE IV
SAR DISTRIBUTIONS FOR THE UTAH MODEL OF THE ADULT MALE WITHOUT SQUISHED EAR FOR COMPARISON WITH DATA OBTAINED BY DIMBYLOW AND MANN USING THE NRPB MODEL [6]. FREQUENCY = 900 MHz. RADIATED POWER = 600 mW. DISTANCE OF THE SOURCE POINT TO THE EAR = 1.38 cm (7δ) AS AGAINST 1.4 cm IN [6]

	No hand λ/4 antenna above handset	No hand λ/2 dipole
Peak 1-voxel SAR (W/kg)	7.57	9.13
Peak 1-g SAR (W/kg)[1]	2.07* (1.00 g; 92.0%)	2.10† (1.00 g; 92.0%)
Peak 1-g SAR (W/kg)[2]	2.49* (1.07 g; 83.0%)	2.71† (1.07 g; 83.0%)
Peak 1-g SAR (W/kg)[3]	2.45* (1.18 g; 86.1%)	2.47† (1.13 g; 81.5%)
Peak 1-g SAR for brain (W/kg)[2]	1.36 (1.01 g)	1.54 (1.01 g)
Peak 1-g SAR for brain (W/kg)[3]	1.31 (1.10 g)	1.48 (1.10 g)
Power absorbed by head and neck	51.7%	52.0%
Peak 1-voxel SAR for brain (W/kg)	4.6	2.6
CSF average (mW/kg)	62.3	60.7
Brain average (mW/kg)	74.4	88.0
Humour average (mW/kg)	50.6	42.8
Lens average (mW/kg)	26.5	19.8
Sclera average (mW/kg)	43.4	33.1

Superscripts 1, 2, and 3 are for cell numbers and subvolumes given in the footnote of Table 3.

* SAR scaled from Table 2 of Reference [6] = 2.17 W/kg.

† SAR scaled from Table 2 of Reference [6] = 2.02 W/kg.

original cells that may occupy the new cell location. The 30° forward-tilted head thus obtained is shown in Fig. 1 together with the original untilted head model. For the tilted model, a vertical orientation of the handset and the antenna allows more accurate modeling of their shapes and dimensions. Models for each of the antennas and the handsets were assumed to be covered with insulating materials of $\varepsilon_r = 4.0$. Because of the different cell sizes used, particularly for the smaller models representative of 10- and 5-year-old children, different values of K_e obtained from (1) have been used for the various simulations for these cases.

Because of the proximity of the hand to the telephone, it is essential to also model the hand for numerical calculations. For the present calculations we have modeled the hand by a region of 2/3 muscle-equivalent material of thickness 1.974 cm ($10\delta_y$) wrapped around the handset on three sides, with the exception of the side facing the head, with height two-thirds that of the handset.

By scaling the cell sizes of the MRI-based model, we have developed smaller models of the head, neck, and hand to correspond to dimensions characteristic of 10- and 5-year-old children, respectively. In the dosimetry handbook [14], the heights and weights for average 10- and 5-year-old children are given as 1.38 and 1.12 m and 32.5 and 19.5 kg, respectively. These heights and weights are also in agreement with the averages for the boys given in [15]. To obtain models of these needed heights, we have scaled the cell size $\delta_z = 3$ mm of the MRI-based model of the adult male of height 176.4 cm to new dimensions $\delta_z = 2.3469$ and 1.9048 mm, respectively. Also, maintaining the square shapes of the pixels in the cross-sectional planes as for the MRI-based model, we have altered the dimensions $\delta_x = \delta_y$ from 1.875 mm of the adult male model of weight 64.0 kg to new cell sizes $\delta_x = \delta_y = 1.51$ and 1.2989 mm to obtain models of 10- and 5-year-old children of weights 32.5 and 19.5 kg, respectively. The approximate hand dimensions have been similarly scaled through these cell sizes so that the hands cover less than two-thirds of the heights of the assumed handsets for models of 10- and 5-year-old children.

It is well-known that considerably lower values of ε_r and σ have previously been reported for fat, bone, and cartilage in the published literature [14], [16] as compared to the higher values that have recently been determined by Gabriel [12]. These lower values of ε and σ reported for fat, bone, and cartilage are given at the bottom of Table II and have been taken instead of the newer values for some of the runs (see Table VI) to determine the effect of tissue properties on SAR distributions.

IV. THE PEAK 1-g SAR

According to the ANSI/IEEE C95.1-1992 RF safety guideline for uncontrolled environments, the spatial-peak SAR should not exceed 1.6 W/kg for any 1 g of tissue defined as a tissue volume in the shape of a cube [1]. Because of

TABLE V
SAR DISTRIBUTIONS FOR THE UTAH MODEL OF THE ADULT MALE WITHOUT SQUISHED EAR FOR COMPARISON WITH DATA OBTAINED BY DIMBYLOW AND MANN USING THE NRPB MODEL [6]. FREQUENCY = 1800 MHz. RADIATED POWER = 125 mW. DISTANCE OF THE SOURCE POINT TO THE EAR = 1.38 cm (7δ) AS AGAINST 1.4 cm IN [6]

	No hand $\lambda/4$ antenna above handset	No hand $\lambda/2$ dipole
Peak 1-voxel SAR (W/kg)	1.54	1.90
Peak 1-g SAR (W/kg)[1]	0.53* (1.00 g; 98.7%)	0.55† (1.00 g; 98.7%)
Peak 1-g SAR (W/kg)[2]	0.87* (1.03 g; 80.0%)	0.81† (1.04 g; 81.0%)
Peak 1-g SAR (W/kg)[3]	0.83* (1.13 g; 81.5%)	0.76† (1.16 g; 83.3%)
Peak 1-g SAR for brain (W/kg)[2]	0.27 (1.04 g)	0.41 (1.01 g)
Peak 1-g SAR for brain (W/kg)[3]	0.27 (1.02 g)	0.40 (1.07 g)
Power absorbed by head and neck	45.4%	46.4%
Peak 1-voxel SAR for brain (W/kg)	0.50	0.64
CSF average (mW/kg)	7.8	9.0
Brain average (mW/kg)	10.4	13.2
Humour average (mW/kg)	8.8	7.4
Lens average (mW/kg)	2.5	2.0
Sclera average (mW/kg)	5.7	4.5

Superscripts 1, 2, and 3 are for cell numbers and subvolumes given in the footnote of Table 3.

* SAR scaled from Table 3 of Reference [6] = 0.70

† SAR scaled from Table 3 of Reference [6] = 0.78.

TABLE VI
SAR DISTRIBUTIONS FOR DIFFERENT PROPERTIES OF THE VARIOUS TISSUES. A $\lambda/4$ ANTENNA ABOVE A HANDSET IS TAKEN FOR THE CALCULATIONS AT 835 MHz. RADIATED POWER = 600 mW

	New properties	Old properties	Homogeneous model
Peak 1-voxel SAR (W/kg)	10.86	8.52	15.98
Peak 1-g SAR (W/kg)	2.93 (1.00 g)	2.05 (1.00 g)	4.17 (1.03 g)
Peak 1-g SAR for brain (W/kg)	1.13 (1.09 g)	0.86 (1.02 g)	---
Power absorbed by head and neck	45.0%	44.0%	41.5%
Power absorbed by "hand"	9.2%	11.9%	8.4%
Peak 1-voxel SAR for brain (W/kg)	1.62	2.11	---
CSF average (mW/kg)	72.7	62.6	---
Brain average (mW/kg)	72.3	62.9	---
Humour average (mW/kg)	31.8	32.9	---
Lens average (mW/kg)	11.3	12.8	---
Sclera average (mW/kg)	17.8	19.4	---

the irregular shape of the body (e.g., the ears) and tissue heterogeneities, a tissue volume in the shape of a cube of, say, $1 \times 1 \times 1$ cm will have a weight that may be in excess of, equal to, or less than 1 g. Larger or smaller volumes in the shape of a cube may, therefore, need to be considered to obtain a weight of about 1 g. Furthermore, for an anatomic model such as ours using unequal cell sizes ($1.974 \times 1.974 \times 3$ mm), it is not very convenient to obtain exact cubical volumes even though nearly cubic shapes may be considered. We have, therefore, considered $5 \times 5 \times 3$, $5 \times 5 \times 4$, and $6 \times 6 \times 3$ cells for the model of the adult male to obtain subvolumes on the order of 1 cm^3. For each of these subvolumes selected close to and around the regions of the high SAR's, we have divided the absorbed powers by the weights calculated for

TABLE VII
COMPARISON OF THE POWERS ABSORBED AND PEAK SAR'S FOR THE $\lambda/4$ AND $3\lambda/8$ ANTENNAS AT 835 MHz. TIME-AVERAGED RADIATED POWER = 600 mW

Antenna length	Tilt	Peak 1-g SAR for Head	Peak 1-g SAR for Brain	% power absorbed by "hand"	% power absorbed by head and neck
$\lambda/4$	0°	2.93 (1.00 g)	1.13 (1.09 g)	9.2	45.0
$\lambda/4$	30°	2.42 (1.03 g)	0.93 (1.02 g)	12.4	39.8
$3\lambda/8$	0°	1.60 (1.00 g)	0.65 (1.05 g)	5.6	33.7

TABLE VIII
COMPARISON OF THE POWERS ABSORBED AND PEAK SAR'S FOR THE $\lambda/4$ AND $3\lambda/8$ ANTENNAS AT 1900 MHz. TIME-AVERAGED RADIATED POWER = 125 mW

Antenna length	Tilt	Peak 1-g SAR for Head W/kg	Peak 1-g SAR for Brain W/kg	% power absorbed by "hand"	% power absorbed by head and neck
$\lambda/4$	0°	1.11 (1.03 g)	0.20 (1.00 g)	13.8	35.6
$\lambda/4$	30°	1.08 (1.03 g)	0.20 (1.04 g)	13.9	35.5
$3\lambda/8$	0°	0.69 (1.06 g)	0.16 (1.00 g)	7.0	29.4

TABLE IX
COMPARISON OF SAR DISTRIBUTIONS FOR MODELS OF AN ADULT MALE AND 10-YEAR AND 5-YEAR-OLD CHILDREN. FREQUENCY = 835 MHz. TIME-AVERAGED RADIATED POWER = 600 mW. A $\lambda/4$ ANTENNA ABOVE A HANDSET IS TAKEN FOR THE CALCULATIONS

	Adult male	10-year-old child	5-year-old child
Peak 1-voxel SAR (W/kg)	10.86	16.82	31.73
Peak 1-g SAR* (W/kg)	2.93 (1.00 g)	3.21 (1.02 g)	4.49 (1.00 g)
Peak 1-g SAR for brain* (W/kg)	1.13 (1.09 g)	1.42 (1.00 g)	1.56 (1.00 g)
Power absorbed by head and neck	45.0%	42.6%	39.5%
Power absorbed by "hand"	9.2%	10.7%	5.5%
Peak 1-voxel SAR for brain (W/kg)	1.62	3.02	4.62
CSF average (mW/kg)	72.7	187.2	283.2
Brain average (mW/kg)	72.3	160.3	239.8
Humour average (mW/kg)	31.8	78.2	117.3
Lens average (mW/kg)	11.3	33.6	52.5
Sclera average (mW/kg)	17.8	48.7	73.7

* $5 \times 5 \times 4$ cells; $0.987 \times 0.987 \times 1.200$ cm; 1.170 cm^3 for the adult male
$7 \times 7 \times 4$ cells; $1.057 \times 1.057 \times 0.939$ cm; 1.049 cm^3 for the 10-year-old child
$8 \times 8 \times 5$ cells; $1.039 \times 1.039 \times 0.950$ cm; 1.026 cm^3 for the 5-year-old child

the individual subvolumes to obtain 1-g SAR's. Furthermore, we have considered only those subvolumes where at least 80 percent of the cells are occupied by the tissues and no more than 20 percent of the cells are in air. As expected, there is a great deal of variability in the 1-g SAR's that are obtained. In keeping with the ANSI/IEEE safety guidelines, weights equal to or in excess of 1 g are considered to obtain the spatial-peak SAR's that are given in Table III.

TABLE X
COMPARISON OF SAR DISTRIBUTIONS FOR MODELS OF AN ADULT MALE AND 10-YEAR and 5-YEAR-OLD CHILDREN. FREQUENCY = 1900 MHz. TIME-AVERAGED RADIATED POWER = 125 mW. A $\lambda/4$ ANTENNA ABOVE A HANDSET IS TAKEN FOR THE CALCULATIONS

	Adult male	10-year-old child	5-year-old child
Peak 1-voxel SAR (W/kg)	3.90	4.90	6.20
Peak 1-g SAR* (W/kg)	1.11 (1.03 g)	0.90 (1.02 g)	0.97 (1.07 g)
Peak 1-g SAR for brain* (W/kg)	0.20 (1.00 g)	0.25 (1.07 g)	0.31 (1.00 g)
Power absorbed by head and neck	35.6%	34.4%	32.2%
Power absorbed by "hand"	13.8%	9.4%	6.8%
Peak 1-voxel SAR for brain (W/kg)	0.29	0.42	0.61
CSF average (mW/kg)	8.0	20.6	33.4
Brain average (mW/kg)	7.6	19.6	32.9
Humour average (mW/kg)	3.2	17.4	39.2
Lens average (mW/kg)	1.5	7.6	17.8
Sclera average (mW/kg)	1.8	9.9	20.5

* $5 \times 5 \times 4$ cells; $0.987 \times 0.987 \times 1.200$ cm; 1.170 cm^3 for the adult male
$7 \times 7 \times 4$ cells; $1.057 \times 1.057 \times 0.939$ cm; 1.049 cm^3 for the 10-year-old child
$8 \times 8 \times 5$ cells; $1.039 \times 1.039 \times 0.950$ cm; 1.026 cm^3 for the 5-year-old child

In Table III it is interesting to note that even though the peak 1-g SAR's for the superficial tissues are highly variable (by almost 2:1), the corresponding values for the internal tissues such as the brain are nearly identical regardless of the subvolumes that are considered. The reason for the highly variable peak 1-g SAR's for the superficial tissues is that various subvolumes of, say, 0.8–1.2 cm^3 in the shape of a cube may each give a weight of about 1 g, depending on the amount of air in such subvolumes. For our case, larger subvolumes such as $5 \times 5 \times 4$ and $6 \times 6 \times 3$ cells with volumes of 1.17 and 1.26 cm^3, respectively, involve more of air and the ear tissues and still have weights of at least 1 g, whereas the smaller subvolumes of $5 \times 5 \times 3$ cells with a total volume of 0.88 cm^3 must have more of the nonear head tissues in order to get weights of 1 or more grams of weight. Since the subvolumes to consider for peak 1-g SAR's have not been clearly defined in the ANSI/IEEE safety guidelines, the variability in the peak 1-g SAR's given in Table III is hard to resolve and is clearly troublesome. All three peak 1-g values have, therefore, been given in Table III. For each of the cases, the weights and percentage of tissues by volume are given within parentheses of the peak 1-g SAR's.

This problem of lack of definition of the subvolume to consider was brought to the attention of the Dosimetry Working Group[2] of Wireless Technology Research. At its meeting in Duarte, California, on October 30, 1995, the working group decided to recommend to ANSI/IEEE that the tissue subvolume to consider should not extend beyond the most exterior surfaces of the body (e.g., the upper, lower, and side boundaries of the ear) but may include the air that is contained therein (e.g., the air in the crevices of the ear). Also, the weight of the subvolume may not be smaller than 1.0 g, but preferably as close to it as possible. For the SAR data given in Table III, this corresponds to case 2 with a peak 1-g SAR of 1.11 W/kg for the $\lambda/4$ antenna and 0.69 W/kg for the $3\lambda/8$ monopole antenna above the handset.

[2]The Dosimetry Working Group of Wireless Technology Research consists of the following individuals: A. W. Guy (Chairman), C. K. Chou, C. Gabriel, O. P. Gandhi, N. Kuster, R. Petersen, P. Polson, V. Santomaa, Q. Balzano, and A. Taflove.

V. TEST RUNS—COMPARISON WITH CALCULATIONS OF DIMBYLOW AND MANN [6]

Even though all of our calculations have been done for plastic-coated handsets and antennas, we have made a limited number of runs using the same configurations as previously used by Dimbylow and Mann [6]. The objective of these runs was to verify that the SAR distributions obtained at 900 MHz and 1800 MHz were fairly similar to those obtained by another research group which had used a very different model of the head and neck. For these test runs we used the tissue properties given in Table II, which were taken from [6] as far as possible, and likewise assumed the handset dimensions of $2.4 \times 6 \times 15$ cm. Unlike the cubical cell sizes of 2 mm used by Dimbylow and Mann [6], we have taken a voxel size of $1.974 \times 1.974 \times 3$ mm for our calculations. The summaries of the results obtained for the four test cases without the hand are given in Tables IV and V for 900 and 1800 MHz, respectively. Also given as footnotes are the data calculated by Dimbylow and Mann [6] for comparison. Since the exact weights of the $1 \times 1 \times 1$ cm subvolume were not prescribed in [6], we have considered the various subvolumes 1, 2, and 3 that were previously considered for the data given in Table III. Also, even though the exact placements of the assumed handset vis à vis the ear were not exactly prescribed in [6], it is interesting to note that the peak 1-g SAR's calculated for our model are fairly similar to Dimbylow's [6] both at 900 and 1800 MHz. For our calculations we have assumed the feed points to be in the cross-sectional plane 6 mm below the top of the ear.

TABLE XI
COMPARISON OF SAR DISTRIBUTIONS FOR MODELS OF AN ADULT MALE AND 10-YEAR AND 5-YEAR-OLD CHILDREN. FREQUENCY = 835 MHz. TIME-AVERAGED RADIATED POWER = 600 mW. A $3\lambda/8$ ANTENNA ABOVE A HANDSET IS TAKEN FOR THE CALCULATIONS

	Adult male	10-year-old child	5-year-old child
Peak 1-voxel SAR (W/kg)	5.97	7.65	12.75
Peak 1-g SAR* (W/kg)	1.60 (1.00 g)	1.49 (1.00 g)	1.88 (1.00 g)
Peak 1-g SAR for brain* (W/kg)	0.65 (1.05 g)	0.78 (1.00 g)	0.85 (1.00 g)
Power absorbed by head and neck	33.7%	28.8%	25.5%
Power absorbed by "hand"	5.6%	4.3%	2.8%
Peak 1-voxel SAR for brain (W/kg)	0.93	1.40	2.01
CSF average (mW/kg)	79.8	170.6	244.5
Brain average (mW/kg)	63.9	125.5	183.0
Humour average (mW/kg)	21.4	46.5	69.8
Lens average (mW/kg)	7.9	20.6	31.2
Sclera average (mW/kg)	12.0	29.3	43.3

* $5 \times 5 \times 4$ cells; $0.987 \times 0.987 \times 1.200$ cm; 1.170 cm^3 for the adult male
$7 \times 7 \times 4$ cells; $1.057 \times 1.057 \times 0.939$ cm; 1.049 cm^3 for the 10-year-old child
$8 \times 8 \times 5$ cells; $1.039 \times 1.039 \times 0.950$ cm; 1.026 cm^3 for the 5-year-old child

TABLE XII
COMPARISON OF SAR DISTRIBUTIONS FOR THE FULL MODEL AND TRUNCATED HALF AND ONE-THIRD MODELS OF THE HEAD AND NECK OF AN ADULT MALE. A $\lambda/4$ ANTENNA ABOVE A HANDSET IS TAKEN FOR THE CALCULATIONS AT 1900 MHz. RADIATED POWER = 125 mW

	Full model	Truncated half model	Truncated One-Third Model
Peak 1-voxel SAR (W/kg)	3.90	3.96	3.96
Peak 1-g SAR (W/kg)	1.11 (1.03 g)	1.11 (1.03 g)	1.11 (1.03 g)
Peak 1-g SAR for brain (W/kg)	0.20 (1.00 g)	0.19 (1.05 g)	0.19 (1.00 g)
Power absorbed by head and neck	35.6%	34.5%	32.4%
Power absorbed by "hand"	13.8%	14.3%	13.3%
Peak 1-voxel SAR for brain (W/kg)	0.29	0.29	0.29
CSF average (mW/kg)	8.0	7.1†	4.8†
Brain average (mW/kg)	7.6	7.3†	6.1†
Humour average (mW/kg)	3.2	3.2†	2.4†
Lens average (mW/kg)	1.5	1.5†	1.5†
Sclera average (mW/kg)	1.8	1.7†	1.4†

† Average over the total mass of tissue in the full model.

VI. EFFECT OF TISSUE PROPERTIES ON SAR DISTRIBUTIONS

As given in Table I with both the old and the new values of dielectric properties, considerably higher values of ε_r and σ have recently been reported for fat, bone, and cartilage by Gabriel [12]. The ear is composed mainly of cartilage that is covered by the skin. In Table VI we compare the salient features of the SAR distributions at 835 MHz that are obtained using both the new and old dielectric properties for these tissues. For this and all further tables we give the SAR's that are calculated using the procedure suggested by the Dosimetry Working Group of WTR [see Section IV].

Since some measurement systems for SAR evaluations use an homogeneous phantom model, also shown for comparison in Table VI are the SAR's obtained for the homogeneous model with properties identical to that of the brain at 835 MHz [see Table II]. It is interesting to note that the homogeneous model overestimates the peak 1-g SAR by 42 percent as compared to that obtained using the anatomically based model.

For each of the calculations given in Table VI, we have considered a quarter-wave monopole antenna above a handset of dimensions $2.96 \times 5.73 \times 15.5$ cm ($14\delta_x \times 28\delta_y \times 51\delta_z$ for the metal covered with 1-mm thick plastic on all sides) and the model of the adult male. The telephone is held against the

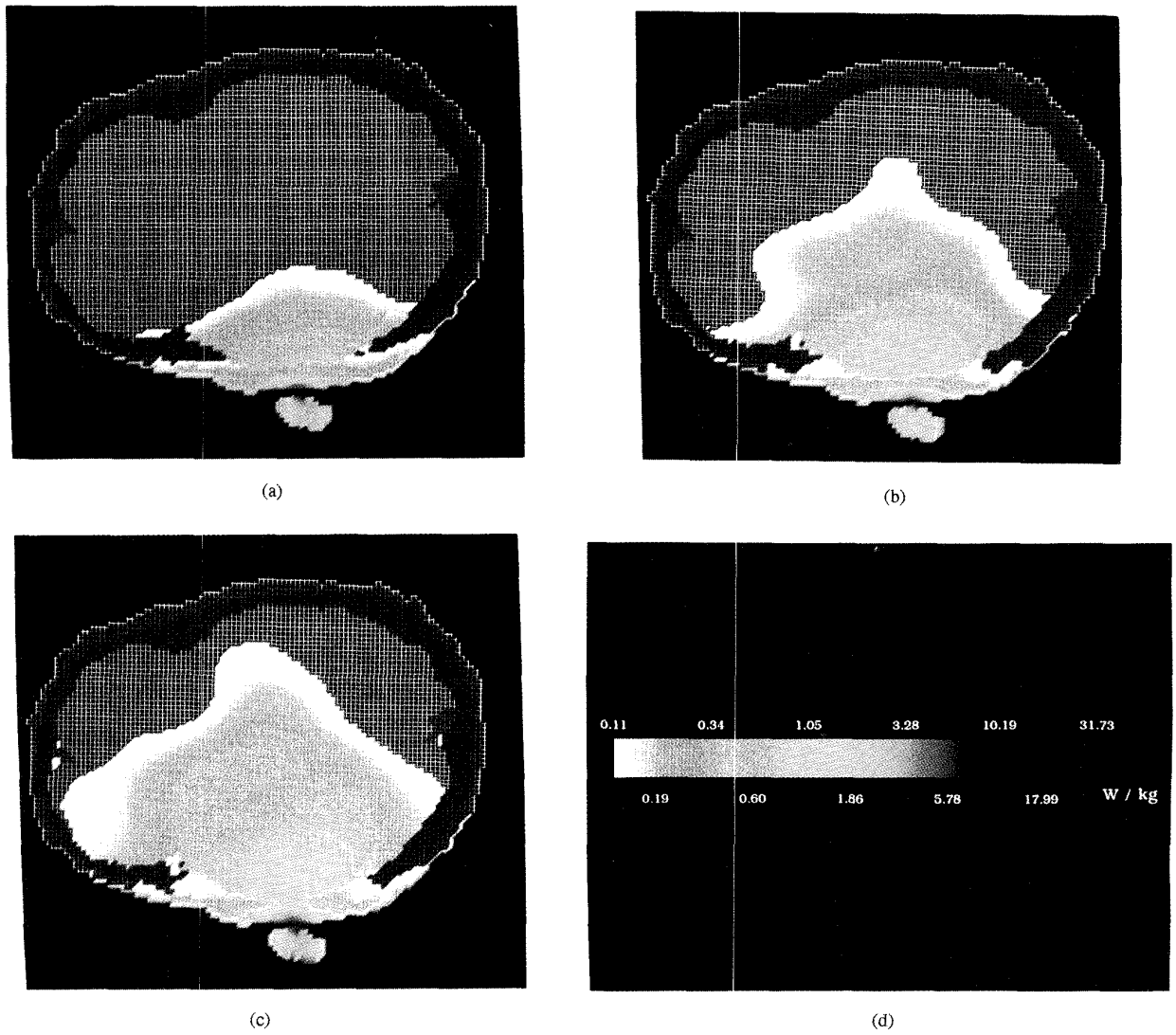

Fig. 2. The SAR distributions for layer no. 34 for models of an adult male and 10-year and 5-year-old children (a)–(c). (d) Scale. This layer contains the feed point and is 2 cells lower than the cross-sectional plane passing through the top of the ear for each of the models. Frequency = 835 MHz. Radiated power = 600 mW.

left side of the head. The driving point of the monopole is located at the top of the handset, in the center of the 5.73-cm side furthest from the ear on the edge of the 2.96-cm side. The thin monopole antenna is embedded in a covering sheath of dielectric material $\varepsilon_r = 4.0$ which, in the FDTD formulation, is modeled by a 2×2 cell square stack of dielectric cells of cross-sectional dimensions 3.95×3.95 mm. New dielectric properties of the various tissues given in Table I are used for the results given in column 1 for these and all further cases considered in this paper.

Even though very similar fractional powers absorbed by the whole head are obtained for all three models, the peak 1-voxel SAR's are considerably higher for the models using the newer higher conductivities for the cartilage. Furthermore, the homogeneous model grossly overestimates the SAR and is also incapable of providing tissue-relevant SAR distributions.

VII. Effect of Antenna Length and Tilt on the SAR Distributions

We have examined the effect of antenna length and its tilt on the power absorbed and the SAR distribution for the various regions of the head and neck. For these studies, two different lengths of the antenna $\lambda/4$ and $3\lambda/8$ and two different orientations of the handset, 0° and 30° relative to vertical, were used for irradiation frequencies of 835 and 1900 MHz. The salient features of the results are given in Tables VII and VIII, respectively. For each of the cases, the handset dimensions are the same as in Section VI ($2.96 \times 5.37 \times 15.5$ cm) and the antennas placed on the back side of the handset similar to Section VI are assumed to be covered by a dielectric sleeve as described in the previous section. It is interesting to note that the powers absorbed by the head and neck and peak 1-g SAR's

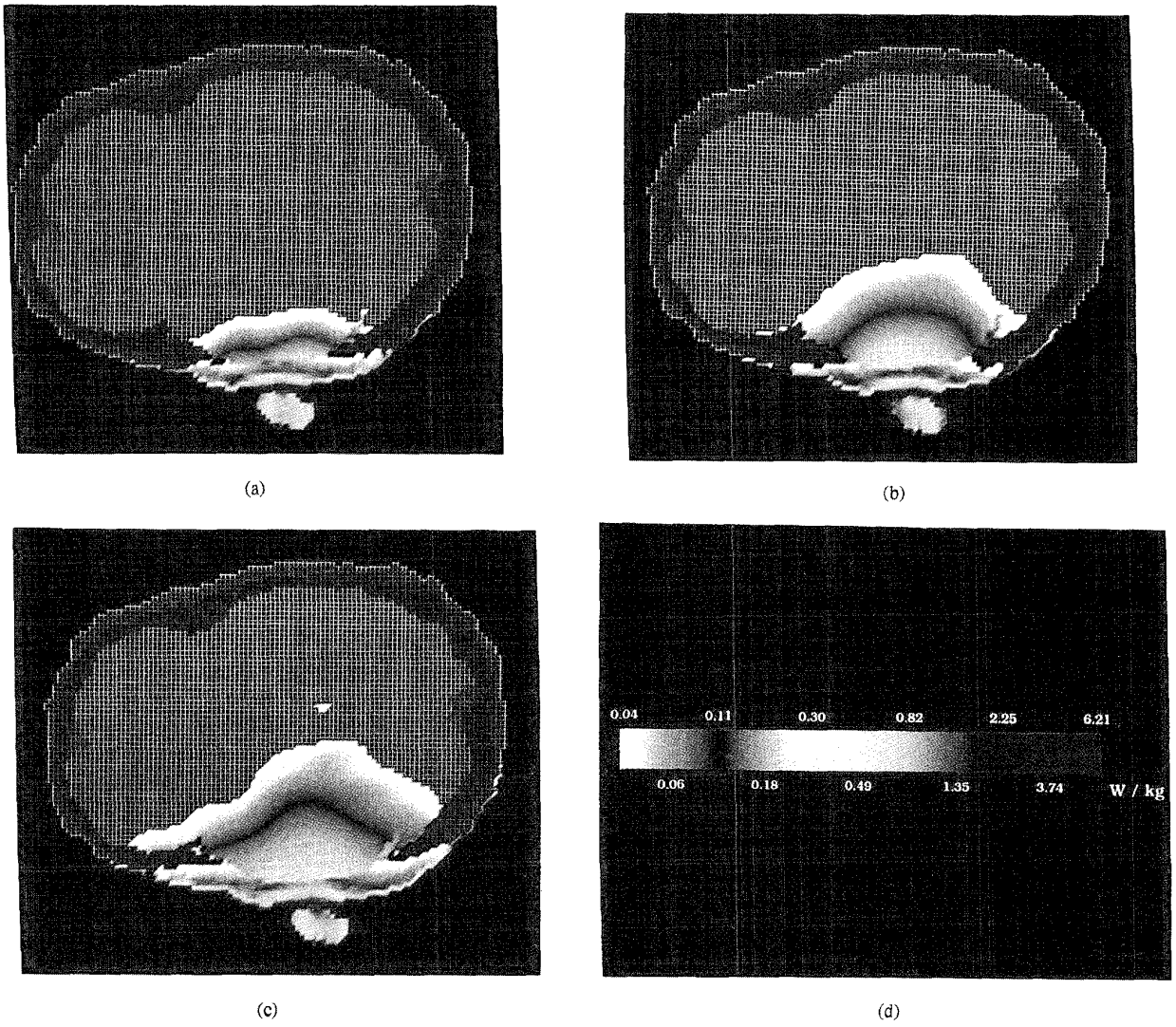

Fig. 3. The SAR distributions for layer no. 34 for models of an adult male and 10-year and 5-year-old children (a)–(c). (d) Scale. This layer is 2 cells lower than the cross-sectional plane passing through the top of the ear for each of the models. Frequency = 1900 MHz. Radiated power = 125 mW.

are lower for $3\lambda/8$ antennas vis à vis $\lambda/4$ antennas both at 835 MHz and 1900 MHz (Tables VII and VIII). This may be due to the fact that $3\lambda/8$ antennas are 50 percent longer than $\lambda/4$ antennas at each of the frequencies. The peak current region for a $3\lambda/8$ antenna is $\lambda/8$ above the feed point, whereas for a $\lambda/4$ antenna it is at the base of the antenna, and, hence, very close to the ear. For the longer $3\lambda/8$ antennas both at 835 and 1900 MHz, the peak current regions are, therefore, somewhat removed from the ear and the head, which results in lower absorbed powers and SAR's than the $\lambda/4$ antenna. Similar arguments can also be given for the calculated lower SAR's for 30° tilted $\lambda/4$ antenna vis à vis the vertically held antenna at 835 MHz (Table VII), since the considerably longer antennas are physically further away from the head, which results in lower SAR's for the tilted antenna, while a similar effect does not occur at the higher frequency of 1900 MHz (Table VIII) because of the smaller length of the antenna.

VIII. Effect of Head Size on SAR Distribution: Comparison for Adult and 10- and 5-Year-Old Children

As previously described in Section III, we have developed smaller models of the head, neck, and "hand" by reducing the voxel size 1.974 × 1.974 × 3.0 mm of the MRI-based model to new voxel sizes of 1.51 × 1.51 × 2.3469 mm and 1.2989 × 1.2989 × 1.9048 mm in order to obtain dimensions characteristic of 10- and 5-year-old children, respectively. In Tables IX and X, we give the salient features of the SAR distributions obtained for quarter-wave monopole antennas mounted as discussed earlier at irradiation frequencies of 835 and 1900 MHz, respectively. It is interesting to note that even though the peak 1-g SAR's are fairly similar for the three models at 1900 MHz, the 1-g SAR's are considerably higher for the smaller head sizes at 835 MHz (Table IX).

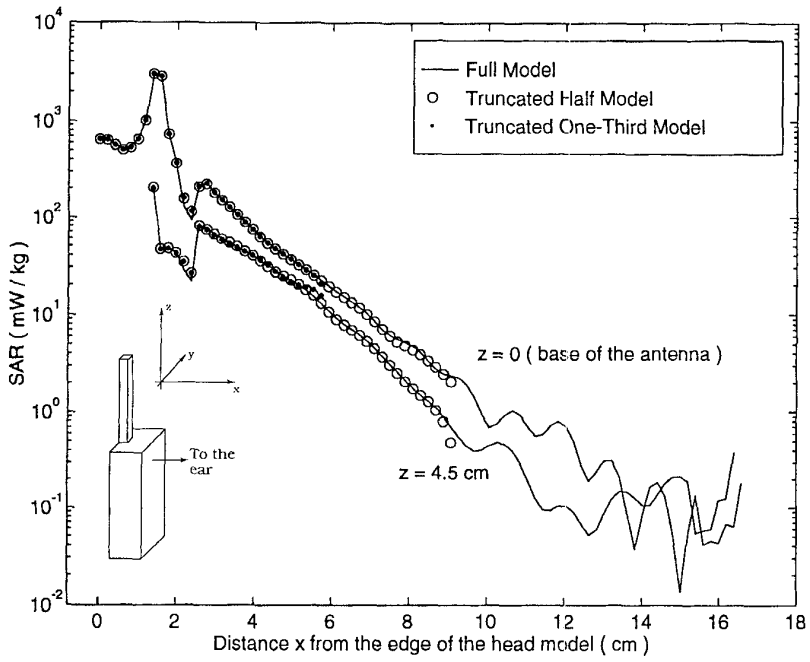

Fig. 4. Comparison of the SAR distributions for the full model and the truncated half and one-third models of the human head along the axis for $z = 0$ and $z = 4.5$ cm for a $\lambda/4$ monopole above the handset. Frequency = 1900 MHz. Radiated power = 125 mW.

Also, the peak 1-voxel SAR's are higher and a larger in-depth penetration of absorbed energy or higher SAR's are obtained for the smaller models both at 835 and 1900 MHz. The fact that there is a larger in-depth penetration of SAR's for the models of 10- and 5-year-old children as compared to those for the model of the adult is illustrated in Figs. 2 and 3 for 835 and 1900 MHz, respectively. Because of a larger depth of penetration of EM field at 835 MHz into the heads of the small subjects, increased SAR's are obtained for smaller models at this frequency. A similar trend of increasing 1-g SAR's for the smaller models at 835 MHz has also been observed for a longer $3\lambda/8$ antenna for which the SAR distributions are given in Table XI. The higher 1-voxel SAR's for the smaller models in Tables IX–XI are likely due to the thinner ears, which results in the antennas being somewhat closer to the region of highest SAR's that are observed generally at the points of contact of the ear pressed against the scalp of the head.

IX. Use of Truncated Head Models for Efficient Computations

With ever-increasing frequencies being considered for wireless communications, it is obvious that even finer-resolution anatomically based models than those being used at the present time will be needed in the future. Since even present models require a lot of computer memory (150–170 Mbytes), the required higher-resolution models will be extremely difficult to use unless more efficient FDTD formulations are developed. We have recently developed a technique to reduce the size of the problem to half or less, recognizing that the distal side of the head is relatively shielded from the EM fields of personal mobile devices. Because of the minuscule coupling, we may place another identical source (a mobile telephone) symmetrically on the opposite side leaving the problem unaltered, provided this dummy source is assumed to be devoid of RF power. This latter assumption can be implemented by exciting the dummy source identically and in phase or out of phase from the actual source for two consecutive simulations and superimposing the EM fields obtained for these even- and odd-mode calculations, respectively. The even-mode simulation can be done by putting a perfect magnetic conductor at the plane of symmetry of the problem and an odd-mode simulation can be done by putting a perfect electric conductor at the same plane of symmetry. Using this approach, only half-problem simulation may be done at a time with a considerable saving of computer memory. To check the validity of this approach, several test cases, including spheres, layered, spheres, etc., were considered for an assumed radiation frequency of 1900 MHz. Excellent agreements of the SAR distributions were obtained for the truncated half and one-third models with those for the full models.

Fig. 4 shows the SAR distributions obtained for an MRI-based model of the human head for which the $\lambda/4$ monopole above a box cellular telephone described earlier in Sections II and VI is placed against the left ear, which is assumed to be squished against the head. The SAR distributions are shown for the model of the head and for truncated half and one-third models for two axes in the x-direction corresponding to $z = 0$, i.e., the plane containing the base of the antenna and $z = 4.5$ cm above this plane. The peak SAR of 3,000 mW/kg for the $z = 0$ line in the plane containing the driving point is due to focusing of induced currents passing at the points of contact between the squished ear and the head. Salient features of the data obtained for this case are given in Table XII. It is

interesting to note that nearly identical SAR's are obtained for the electromagnetically coupled region in proximity to the telephones for each of the models. Because of the truncation of the models, somewhat lower SAR's are obtained for the more distal tissues for which the SAR's are fairly small anyway. The difference in the peak and 1-g average SAR's calculated using the full and the truncated models is less than 1.5 percent.

X. Concluding Remarks

The previously tested finite-difference time-domain method has been used with a new MRI-based millimeter-resolution model of the human to study electromagnetic energy absorption in the head and neck due to mobile telephones at 835 and 1900 MHz. We have used dimensions of the handsets that are characteristic of the newer telephones to obtain SAR distributions due to two different lengths of the monopole antennas of lengths $\lambda/4$ and $3\lambda/8$. As expected, the longer antennas give SAR's that are considerably smaller than those for $\lambda/4$ antennas. A limited number of test runs using the antennas and handset dimensions previously used by Dimbylow and Mann [6] give 1-g SAR's that are very similar (within 10 percent) to those obtained by these authors. This is most interesting since considerably different anatomically based models of the human head and neck have been used. We have also examined the effect of using the widely different tissue properties that have been reported for fat, bone, and cartilage. As expected, the new higher conductivities and dielectric constants recently reported for these tissues give peak 1-voxel and 1-g SAR's that are higher than those obtained with the previously reported lower electrical properties. Use of a homogeneous brain-equivalent model is shown to grossly overestimate peak SAR's for 1-voxel as well as for 1-g of tissue. To represent typical usage, we have studied the effect of tilting the telephone relative to the head at an angle of 30°. Because of the longer antenna at 835 MHz, this results in a reduction of SAR's relative to the untilted configuration, since the antenna is now further away from the head for much of its length. This effect is inconsequential at 1900 MHz, where the antenna length is fairly small.

A highlight of this paper has been to calculate SAR distributions using reduced-scale models of the head and neck and "hand" to correspond to the dimensions that are characteristic of 10 and 5-year-old children. Because of the deeper penetration of EM energy in smaller models, considerably higher internal tissue SAR's are obtained both at 835 and 1900 MHz. Also, higher 1-g SAR's are obtained at 835 MHz for both $\lambda/4$ and $3\lambda/8$ antennas. Lastly, we have shown it possible to use truncated one-half and one-third models of the head and neck and obtain SAR distributions that are nearly identical to those for full models. Use of truncated models allows considerable savings in computer memory and computation time for SAR distributions.

Acknowledgment

The authors thank V. Pandit for assistance with computer graphical displays of the data given in Figs. 1–3, and the University of Utah Supercomputing Institute for a generous use of computer time.

References

[1] ANSI/IEEE C95.1-1992, *American National Standard—Safety Levels with Respect to Exposure to Radio Frequency Electromagnetic Fields, 3 kHz to 300 GHz*. New York: IEEE.

[2] O. P. Gandhi, "Some numerical methods for dosimetry: Extremely low frequencies to microwave frequencies," *Radio Sci.*, vol. 30, pp. 161–177, 1995.

[3] O. P. Gandhi, J. Y. Chen, and D. Wu, "Electromagnetic absorption in the human head for mobile telephones at 835 and 1900 MHz," in *Proc. Int. Symp. Electromag. Compat.*, (EMC'94 Roma), Sept. 13–16, 1994, pp. 1–5.

[4] O. P. Gandhi and J. Y. Chen, "Electromagnetic absorption in the human head from experimental 6-GHz handheld transceivers," *IEEE Trans. Electromag. Compat.*, vol. 37, pp. 547–558, Nov. 1995.

[5] M. A. Jensen and Y. Rahmat-Samii, "EM interaction of handset antennas and a human in personal communications," in *Proc. IEEE*, 1995, vol. 83, pp. 7–17.

[6] P. J. Dimbylow and S. M. Mann, "SAR calculations in an anatomically based realistic model of the head for mobile communication transceivers at 900 MHz and 1.8 GHz," *Physics in Medicine Biology*, vol. 39, pp. 1537–1553, 1994.

[7] K. S. Kunz and R. J. Luebbers, *The Finite-Difference Time-Domain Method in Electromagnetics*. Boca Raton, FL: CRC, 1993.

[8] A. Taflove, *Computational Electrodynamics: The Finite-Difference Time-Domain Method*. Dedham, MA: Artech House, 1995.

[9] J. C. Lin and O. P. Gandhi, "Computational methods for predicting field intensity," in *CRC Handbook Biological Effects Electromag. Fields*, 2nd ed., C. Polk and E. Postow, Eds.. Boca Raton, FL: CRC, ch. 9, pp. 335–399, 1995.

[10] S. Berntsen and S. N. Hornsleth, "Retarded time absorbing boundary conditions," *IEEE Trans. Antennas Propagat.*, vol. 42, pp. 1059–1064, 1994.

[11] R. Luebbers, L. Chen, T. Uno, and S. Adachi, "FDTD calculation of radiation patterns, impedance, and gain for a monopole antenna on a conducting box," *IEEE Trans. Antennas Propagat.*, vol. 40, pp. 1577–1582, 1992.

[12] C. Gabriel, personal communication.

[13] G. Lazzi and O. P. Gandhi, "Realistically tilted and truncated anatomically based models of the human head for dosimetry of mobile telephones," submitted to *IEEE Trans. on Electromag. Compat.*

[14] C. H. Durney, H. Massoudi, and M. F. Iskander, *Radiofrequency Radiation Dosimetry Handbook*, 4th ed., USAF SAM-TR-85-73, USAF School of Aerospace Medicine, Aerospace Med. Div. (AFSC), Brooks Air Force Base, TX, 78235-5301, Oct. 1986.

[15] C. Lentner, Ed., *Geigy Scientific Tables*, CIBA-GEIGY Limited, Basle, Switzerland, 1984.

[16] M. A. Stuchly and S. S. Stuchly, "Dielectric properties of biological substances—Tabulated," *J. Microwave Power*, vol. 15, pp. 19–26, 1980.

Om P. Gandhi (S'57–M'58–SM'65–F'79) is Professor and Chairman, Department of Electrical Engineering at the University of Utah, Salt Lake City. He is the author or co-author of several book chapters, and journal articles on electromagnetic dosimetry, microwave tubes, and solid-state devices. He also edited the book, *Biological Effects and Medical Applications of Electromagnetic Energy* (Prentice-Hall, 1990), and coedited the book, *Electromagnetic Biointeraction* (Plenum Press, 1989).

Dr. Gandhi was elected a Fellow of the IEEE in 1979 and received the Distinguished Research Award from the University of Utah for 1979–1980. He has been President of the Bioelectromagnetics Society (1992–93), Cochairman of the IEEE SCC 28.IV Subcommittee on the RF Safety Standards (1988–), and Chairman of the IEEE Committee on Man and Radiation (COMAR) for 1980–1982. In 1995, he received the d'Arsonval Medal of the Bioelectromagnetics Society for pioneering contributions to the field of bioelectromagnetics. His name is listed in *Who's Who in the World, Who's Who in America, Who's Who in Engineering, and Who's Who in Technology Today.*

Gianluca Lazzi (S'94, M'95) was born in Rome, Italy, on April 25, 1970. In 1994, he received the Dr.Eng. degree in Electronics from the University of Rome "La Sapienza," Rome, Italy. In 1988, he was co-author of the educational software packages used by RAI (Italian National Television) for pilot experiments of transmission of software via television network in Italy. He worked as a consultant for some companies, and in 1994 he joined the Innovation Department of ENEA (Italian National Board for New Technologies, Energy and Environment) where he was involved in the study of electromagnetic compatibility problems. In 1994 he also worked in collaboration with the Department of Electronic Engineering of the University of Rome "La Sapienza." In 1995, he joined the Department of Electrical Engineering at the University of Utah, Salt Lake City, Utah, USA, where he is currently working toward the Ph.D. degree. His principal research interest is the development and the application of numerical techniques (FDTD, MoM) for the analysis of passive planar components, antennas, and the interaction between EM fields and biological media.

Dr. Lazzi is a member of the New York Academy of the Sciences (NYAS) and a member of the Italian Electrical and Electronic Society (AEI). He is winner of the 1996 URSI "Young Scientist Award" and the 1996 "Curtis Carl Johnson Memorial Award" for the best student paper presented at the Annual Technical meeting of the Bioelectromagnetics Society.

Cynthia M. Furse (S'85–M'87) was born in Stillwater, ME, May 7, 1963. She received the B.S.E.E. degree with a mathematics minor magna cum laude in 1986, M.S.E.E. degree in 1988, and Ph.D. degree in 1994, all from the University of Utah.

Her research interests include applying numerical methods to electromagnetic interaction problems, parallel computation for large-scale applications, and high-resolution modeling of the human body for both low- and high-frequency bioelectromagnetic applications. She has worked as a Research Scientist for Chevron Oil Field Research Company, and as a Teaching Assistant and Research Associate at the University of Utah. She is currently a Research Assistant Professor at the University of Utah, studying cellular telephone interaction with the human body, low-frequency bioelectromagnetics, and parallelization of the FDTD code. She teaches "Numerical Techniques in Electromagnetics" and "Electrical Engineering for Third Graders."